Theory of thermopower in disordered mixed crystals: Application to Si-Ge systems

P. J. Lin-Chung and A. K. Rajagopal
Naval Research Laboratory, Washington, D.C. 20375-5347
(Received 23 September 1998; revised manuscript received 11 March 1999)

A Green's-function theory of thermoelectric power in disordered mixed crystals is presented. This theory incorporates features of (a) disorder, (b) band structure, (c) relevant dielectric function, and (d) electron-phonon interaction. By formulating the theory in coordinate space, besides subsuming previous work on metals and alloys as special cases, the inclusion of disorder effects based on coherent potential approximation has been incorporated into this scheme. This formulation gives the concentration and band occupancy dependence of thermopower. Thus it provides a possibility for investigating other disordered mixed systems which may be tailored to yield larger values of thermoelectric figure of merit. As an illustration of this formalism, numerical estimations of the contributions due to disorder and electron-phonon effects to the thermopower in a two-band model of Si-Ge mixed crystal system are given at room temperature. [S0163-1829(99)00441-5]

I. INTRODUCTION

In recent years there has been renewed interest in searching for novel materials that may be used for efficient, environmentally sound cooling and power generation purposes. This has naturally led to research on new materials exhibiting high thermoelectric efficiencies. The performance of a thermoelectric material is characterized by the three important transport coefficients—electrical, thermal, and thermoelectric. A high ratio of electrical to thermal conductivity as well as large thermoelectric power are needed in selecting materials for both thermoelectric generation and refrigeration. Two of the central areas in this search have been the effects of confinement in low dimensional materials in giving improved electric contribution to the thermoelectric transport properties, and the role of disorder in decreasing the lattice thermal conductivity and affecting thermoelectric transport coefficients. Only recently the effect of disorder scattering on thermoelectric materials was reported.[1]

The theory of electrical and thermal transport was given by Kubo and co-workers[2,3] in terms of various correlation functions. This was extended to superconducting systems by Kadanoff and Martin.[4] Luttinger[5] gave a unified ''mechanical'' description of the ''Kubo'' formula for all the transport coefficients. Only recently Jonson and Mahan[6] (JM) worked out in detail these transport coefficients for a free-electron model of simple metals, including electron-phonon interactions. However, the materials of interest in the search for improved thermoelectrics typically are semiconductors and heterostructure systems which have complex crystal structures possessing multiple bands, which cannot be described by these theoretical frameworks. Thus a formulation applicable to realistic systems is needed in the study of semiconducting thermoelectric materials. The purpose of this paper is to provide such a formalism which incorporates (a) disorder, (b) band structure, (c) appropriate dielectric function, and (d) electron-phonon interaction. This is accomplished in Sec. II. In Sec. II A, a general operator formalism for thermal transport in the spirit of Kadanoff and Martin[4] and Luttinger[5] is given. This formalism is in coordinate space and is a representation-free framework. It can be applied to a system possessing localized or extended states. For example, from this formalism the previous result of JM follows by a choice of free-electron representation. Also it is found that the choice of Bloch or Wannier representation in this operator formalism will produce an appropriate description of semiconductors including disorder effects. In Sec. II B, the theory of thermopower of solids is expressed in terms of Kubo response functions.

In Sec. III, the incorporation of disorder effects is given in detail. Disorder occurs not only in bulk alloys but also at the interfaces of heterostructure materials.[7] It is believed this will play an important role for the application of new nanostructure materials because the effect of disorder scattering is of importance in comparison with that of lattice scattering in the consideration of electrical and thermal conductivities.[8–10] However, the thermoelectric power in disordered mixed crystals does not seem to have been examined with the same rigor as for simple metals.[6] This may be due to the fact that the correlation function expression for thermoelectric power tensor involves both charge current and energy current components, which are more complicated. Effects of disorder on the transport phenomena has been considered previously on metallic alloys. Single band, single-site coherent-potential approximations (CPA) are used commonly in studying these systems.[8] For semiconducting disordered systems these approximations can no longer be applied because of the existence of energy gap and the presence of at least two basis atoms per unit cell which introduce multiple bands and create charge transfers between these bands when the impurity effects are included. Here, in order to obtain the self-energy in the disordered semiconducting materials, a generalized CPA formalism[11] applicable to multiband system is used. A Green's-function technique to treat electrons interacting with phonons is also incorporated.

In Sec. IV, a useful special case of the formalism developed here is given to study the thermopower of disordered crystals of the type ($A_{1-c}B_c$) as function of the impurity concentration **c** and as function of the occupation of the bands. Unlike the work on simple metals,[6] several unique features of semiconducting materials such as the nonparabolicity of the energy bands with band gap, the semiconductor

 ©1999 The American Physical Society

dielectric function,[12–14] different from that of the free-electron gas, and the multiband electronic structure including mixed-crystal features of the disordered system are incorporated. These are given in separate Secs. IV A, B, and C.

In Sec. V, an important example of this type of $(A_{1-c}B_c)$ alloy, $Si_{1-c}Ge_c$, is considered in some detail. The choice of this type of material for the present study is because of the suggestions of possible high-temperature thermoelectric material. More recently there are theoretical expectations[15,16] that such a material may exhibit enhanced thermoelectric figure of merit in its superlattice structure. Moreover, the electron and phonon excitation properties of such material have also been investigated for some time,[17–19] which indicates a model for computation in a realistic manner. The concentration dependence of the self-energy is given in Sec. V A, disorder contribution in Sec. V B, dependence of various parts of the product $(\sigma\alpha)$ on concentration and bandfilling in Sec. V C, and a discussion of the numerical results in relation to some experimental results at room temperature in Sec. V D. A summary of the results obtained is given in Sec. VI.

II. THEORETICAL DEVELOPMENT

A. Operator formalism for a combined electron-phonon system

Following Refs. 4 and 5, the energy–current-density operator for a system of electrons and phonons with first-order electron-phonon interaction term included is first constructed. The correlation function of charge–current-density operator and energy–current-density operator is then examined by separating the contributions from electron, phonon, and electron-phonon interaction terms. Thus the correlation function expressions for the thermal transport coefficients obtained here are more general than those derived based on a transport equation.[20] The linear response of a system to an external electric field leads unambiguously to the Kubo formula for the electrical conductivity tensor.[2] This derivation based on a ''well defined Hamiltonian'' is thus ''mechanical.''[5] For a long time, there existed no mechanical formulation for thermal transport problems since there was no Hamiltonian describing a thermal gradient. Green-Kubo-Mori formulas for the thermal transport coefficients are derived based on the assumptions that local variables are controlled either by a Markoff process or by a ''local equilibrium distribution.'' These derivations, while not rigorous, are found to be quite practical. They have been used widely in studying thermal transport. Luttinger[5] gave an essentially mechanical derivation by introducing an inhomogeneous gravitational field which produces the energy flow and temperature fluctuations. A term which appears in the Hamiltonian as a product of this field and the local energy density operator $h(\mathbf{r},t)$ of the system was introduced and a Kubo-type theory was developed by him.

The energy-current operator $j^E(\mathbf{r},t)$ which appears in the correlation functions is determined through the equation of continuity

$$\dot{h}(\mathbf{r},t)+\nabla\cdot j^E(\mathbf{r},t)=0. \tag{1}$$

The overdot represents the time derivative.

Kadanoff and Martin[4] derived $j^E(\mathbf{r},t)$ for superconducting electrons and expressed the correlation functions in terms of a two-particle Green's function familiar in many-body theory. Hardy[21] derived $j^E(\mathbf{r},t)$ for a lattice system. Luttinger gave an expression for a free-electron system.[5] Using the Bloch representation for electrons, Lyo[22] and Vilenkin and Taylor[23] obtained an expression for the energy current. These authors also included electron-phonon interaction contributions. In the present work, $j^E(\mathbf{r},t)$ for a combined electron and phonon system in a representation free form is given. By choosing appropriate representation for the field operators, the expressions found in the literature are obtained as special cases.

The Hamiltonian of the system considered here is

$$H=H_e+H_{ph}+H_{ep}, \tag{2}$$

where

$$H_e=\int d^3\mathbf{r}\,\hat{\psi}^+(\mathbf{r},t)\left[\frac{\hat{p}^2}{2m}+V(\mathbf{r})\right]\hat{\psi}(\mathbf{r},t), \tag{3}$$

$$H_{ep}=-\sum_{\alpha,l}\int d^3\mathbf{r}\,\hat{\psi}^+(\mathbf{r},t)Q_\alpha(l,t)\nabla_\alpha V(\mathbf{r}-\mathbf{R}_l)|_{\mathbf{R}_l=\mathbf{R}_l^0}\hat{\psi}(\mathbf{r},t), \tag{4}$$

$$H_{ph}=\sum_{\alpha,l}\frac{P_\alpha^2(l,t)}{2M(l)}+\frac{1}{2}\sum_{\alpha,\alpha',l,l'}\Phi_{\alpha\alpha'}(l,l')Q_\alpha(l,t)Q_{\alpha'}(l',t), \tag{5}$$

$$V(\mathbf{r})=\sum_l V_l(\mathbf{r}-\mathbf{R}_l^0). \tag{6}$$

$V(\mathbf{r})$ is the static periodic crystal potential giving rise to the band structure for the electrons. $\hat{\psi}^+(\mathbf{r},t)$, $\hat{\psi}(\mathbf{r},t)$ are, respectively, the creation and annihilation field operators for the electrons. $\hat{p}$, $P_\alpha(l,t)$ are the momentum operators for electrons and ions, respectively. $Q_\alpha(l,t)$ is the displacement operator for the ion. m, $M(l)$ are the masses for electrons and ions, respectively. $\mathbf{R}_l$ are the position vectors of vibrating ions with their equilibrium positions at $\mathbf{R}_l^0$. $\Phi_{\alpha\alpha'}(l,l')$ is the dynamical matrix of the vibrating lattice. All these operators are in the Heisenberg representation, and obey equal-time canonical commutation rules. For the sake of simplicity harmonic approximation for the vibrating lattice and the leading-order electron-ion interaction are considered here.

A general expression for $j^E(\mathbf{r},t)$ will be derived by using the definition of $h(\mathbf{r},t)$ in the form

$$h(\mathbf{r},t)=\left[-\frac{\hat{p}_1\cdot\hat{p}_2}{2m}+V(\mathbf{r})\right]\hat{\psi}_1^+\hat{\psi}_2 -\sum_{\alpha,l}\hat{\psi}^+(\mathbf{r},t)Q_\alpha(l,t)\nabla_\alpha V(\mathbf{r}-\mathbf{R}_l)|_{\mathbf{R}_l=\mathbf{R}_l^0}\hat{\psi}(\mathbf{r},t). \tag{7}$$

In the above equation and subsequent equations, the indices, 1 or 2, denote the corresponding variables as $\mathbf{r}_1$, $\mathbf{r}_2$, respectively, and in Eq. (7), we let $\mathbf{r}_1=\mathbf{r}_2=\mathbf{r}$ at the end of the indicated operations.

Equation (1) can also be written as

$$-i\hbar\nabla\cdot j^E(\mathbf{r},t)=[h(\mathbf{r},t),H] \tag{8}$$

by using the standard quantum-mechanical expression for the time derivative of an operator. Here H is the total Hamiltonian operator given by Eq. (2).

From Eqs. (3)–(8) the energy-current operator is derived and may be expressed as a sum of two terms arising from the electron and the electron-phonon interaction. Because the part of energy-current operator arising from phonons only contributes to the correlation function related to the lattice thermal conductivity, and does not contribute to the thermoelectric power, it will not be considered in the following sequel.

It is found that

$$j^E(\mathbf{r},t)=j^E_e(\mathbf{r},t)+j^E_{ep}(\mathbf{r},t), \tag{9}$$

where

$$j^E_e(\mathbf{r},t)=\left(-\frac{\hat{p}_1\cdot\hat{p}_2}{2m}+V(\mathbf{r})\right)\frac{\hat{p}_1-\hat{p}_2}{2m}\hat{\psi}^+_2\hat{\psi}_1, \tag{10}$$

$$\begin{aligned}j^E_{ep}(\mathbf{r},t)=&-\sum_{\alpha,l}[(\nabla_\alpha V(\mathbf{r}-\mathbf{R}^0_l))Q_\alpha(l,t)]\mathbf{j}(\mathbf{r},t)\\&-\frac{i\nabla_r}{4\pi}\sum_{\alpha,l}\int d^3\mathbf{r}'\\&\times(\nabla_\alpha V(\mathbf{r}'-\mathbf{R}^0_l))\frac{\dot{Q}_\alpha(l,t)\rho(\mathbf{r}',t)}{|\mathbf{r}-\mathbf{r}'|},\end{aligned} \tag{11}$$

also

$$\begin{aligned}j(\mathbf{r},t)&=\frac{1}{2mi}[\hat{\psi}^+_2\nabla_1\hat{\psi}_1-(\nabla_2\hat{\psi}^+_2)\hat{\psi}_1]\\&=\frac{\hat{p}_1-\hat{p}_2}{2m}\hat{\psi}^+_2\hat{\psi}_1,\end{aligned} \tag{12}$$

$$\rho(\mathbf{r},t)=\hat{\psi}^+\hat{\psi}, \tag{13}$$

where $j(\mathbf{r},t)$ and $\rho(\mathbf{r},t)$ are, respectively, the electric current density and charge density. The second term in Eq. (11) arises from the commutator of H_{ph} with $h(\mathbf{r},t)$ and the relation $M(l)\dot{Q}_\alpha(l,t)=P_\alpha(l,t)$.

From these equations, the expressions given in the literature[6,22,23] are deduced by expressing the electron field operators $\hat{\psi}(\mathbf{r},t),\hat{\psi}^+(\mathbf{r},t)$ in terms of free-electron states or the appropriate Bloch states associated with the pertinent electron system of metals and alloys. Wannier representation $\{u_m(\mathbf{r})\}$ is found to be convenient for treating site disordered mixed-crystal systems.[1] In semiconductors, alternatively, an effective-mass representation may be used.

B. Theory of thermoelectric power of solids

Several techniques and approximations have been used in the past to develop theories of thermoelectric power. Existing works on thermoelectric power are mostly based on solving the Boltzmann equation in the relaxation-time approximation by a variational method.[24,25] However, the Boltzmann transport equation[20] is for weak scattering and is valid in the dilute-alloy limit. In order to treat more general disordered alloy systems for a wide range of scattering strengths and for all impurity concentrations, correlation function expressions for the transport coefficients are more appropriate. In this context, the Green's-function method is often the technique of choice. More recently, Jonson and Mahan[6] examined the electron-phonon contribution to the thermopower of metals, using a Green's-function technique as in Ref. 4, with harmonic approximation for the phonons.

Here a general formalism applicable not only to metals but also to semiconductors is given. Using the linear response theory of Kubo, Yokota, and Nakajima,[3] the electric and heat currents in terms of the external electric field ($\mathbf{E}$) and temperature gradient ($\boldsymbol{\nabla}T$) are expressed in the form

$$\begin{pmatrix}\dfrac{-\mathbf{j}}{e}\\[2ex]\dfrac{-\mathbf{j}^Q}{kT}\end{pmatrix}=\begin{pmatrix}\dfrac{\sigma}{e^2}&\dfrac{\sigma\alpha}{ek}\\[2ex]\dfrac{\sigma\alpha}{ek}&\dfrac{\kappa+T\sigma\alpha^2}{k^2T}\end{pmatrix}\begin{pmatrix}e\mathbf{E}\\\boldsymbol{\nabla}(kT)\end{pmatrix}. \tag{14}$$

Here σ is the electrical conductivity tensor, κ is the thermal conductivity tensor at zero electric current, and $\sigma\alpha$ is the tensor product of the electrical conductivity and the thermopower α. Based on the Green-Kubo-Mori formula this product is given in terms of the correlation function by

$$\begin{aligned}(\sigma\alpha)_{\mu\nu}(\omega)=&\lim_{\eta\to0^+}\frac{1}{\Omega}\int_0^\infty dt\,e^{-i\omega t-\eta t}\\&\times\int_0^\beta d\lambda\langle j_\mu(0)j^Q_\nu(t+i\hbar\lambda)\rangle.\end{aligned} \tag{15}$$

$j_\mu(0)$ is the total electric current and is given by integrating Eq. (12) over all space. $j^Q_\nu(t)$ is the total heat current which is related to the energy current by $j^Q(t)=j^E(t)-\mu j(t)$. Here μ is the chemical potential. β is the inverse temperature, $(kT)^{-1}$. The contributions to the thermopower in Eq. (15) then contain the following three types of correlation functions:

$$\langle j_\mu(0);j_\nu(t)\rangle\approx\langle c^+_1(0)c_2(0);c^+_3(t)c_4(t)\rangle, \tag{16}$$

$$\langle j_\mu(0);j_\nu(t)Q_\alpha(l,t)\rangle\approx\langle c^+_1(0)c_2(0);c^+_3(t)c_4(t)Q_\alpha(l,t)\rangle, \tag{17}$$

$$\langle j_\mu(0);\rho_\nu(t)\dot{Q}_\alpha(l,t)\rangle\approx\langle c^+_1(0)c_2(0);c^+_3(t)c_4(t)\dot{Q}_\alpha(l,t)\rangle, \tag{18}$$

the first of which is similar to that appearing in the exact expression for electrical conductivity tensor $\sigma_{\mu\nu}(\omega)$:[2]

$$\sigma_{\mu\nu}(\omega)=\lim_{\eta\to0^+}\frac{1}{\Omega}\int_0^\infty e^{-i\omega t-\eta t}dt\int_0^\beta d\lambda\langle j_\mu(0)j_\nu(t+i\hbar\lambda)\rangle. \tag{19}$$

The second and third expressions in Eqs. (17) and (18) appear only for thermopower, because of the inclusion of the electron-phonon interaction. Procedures for decoupling the configuration averaged two-particle Green's functions into products of two one-particle Green's functions as an approximation[26] can be generalized to determine the contributions in Eqs. (17) and (18) through the conversion of pho-

non displacement operators into electron operators using the following equation of motion for the combined electron-phonon system:

$$Q_\alpha(l,t)=M^{-1}\sum_{\alpha',l',m,m'}\int D_0(\alpha l t;\ \alpha' l' t')\nabla_{\alpha'}V(\mathbf{r}-\mathbf{R}_l^0)\times u_m^*(\mathbf{r})u_{m'}(\mathbf{r})c_m^+(t')c_{m'}(t')dt'd^3\mathbf{r},\qquad(20)$$

where D_0 is the bare phonon Green's function. In the case of metals, these expressions were examined by JM when the electron field operators were expressed in terms of the free-electron operators. Because the evaluation of the transport coefficients relies upon the determination of the one-particle Green's functions, the configuration-averaged Green's function in a homogeneous random disordered system is crucial in the study of disordered mixed crystals. In the adiabatic approximation, the time derivative of the phonon displacement operator in Eq. (18) is ignored. In the next section, a theory for disordered systems for multiband semiconductors is developed.

III. MULTIBAND COHERENT-POTENTIAL APPROXIMATION FOR DISORDERED MIXED CRYSTALS

In the study of disordered mixed crystals only idealized models have been considered. Such results for simple systems are valuable, both in guiding physically motivated approximations and in finding unusual features unique to the disordered systems. CPA (Refs. 27–29) is one of the most powerful techniques used in the calculations of electrical conductivity[8] and lattice thermal conductivity[10] of disordered binary alloys. This technique is capable of dealing with single particle properties of elementary excitations in site-disordered crystals of the type A_cB_{1-c} for arbitrary c, and for moderately different characteristics of A and B within the framework of multiple-scattering theory. It may be regarded as an interpolation scheme between properly described limits corresponding to the entire range of impurity concentration and strong and weak scattering.

Velicky[8] used a single band model Hamiltonian to describe the electronic structure of a disordered binary alloy. The single-site approximation in a multiple-scattering description then was used by him for the evaluation of the electrical conductivity. In the single band CPA, it is essential to restrict the disorder to be site-diagonal in order to simplify the treatment. In this case an effective medium scheme is obtained which contains effective atoms each having self-energy Σ. The averaged Green's function G is related to the self-energy Σ by

$$G(z)=[z-E(k)-\Sigma]^{-1},\qquad(21)$$

where $E(k)$ is the periodic part of the Hamiltonian. $\Sigma(z)$ is the electron self-energy in the presence of disorder scattering and is determined self-consistently by the following equation specifying no scattering on the average from any site n in the effective medium.[26] The Wannier representation is used in describing this approximation, and then using the relationship to the Bloch representation via the lattice Fourier transformation, we obtain

$$|k\rangle=N^{-1/2}\sum_n e^{i\mathbf{k}\cdot\mathbf{R}_n}|n\rangle,\qquad(22)$$

$$\Sigma(z)=E_{\rm av}+c(1-c)\Delta^2\frac{F(z)}{1+[\Sigma(z)+E_{\rm av}]F(z)}.\qquad(23)$$

Here $F(z)=\langle n|G(z)|n\rangle=N^{-1}\sum_k G(k,z)$ (24)

is the site-diagonal matrix element of the averaged Green's function, Eq. (21), in the Wannier representation which is also expressed in the Bloch representation as indicated above.

$E_{\rm av}$ is defined as

$$E_{\rm av}\equiv cE^A+(1-c)E^B.\qquad(25)$$

E^A, E^B are the diagonal matrix elements of the Hamiltonian with respect to the Wannier representation for pure crystals A and B, respectively. The energy zero is defined such that

$$E^A=-E^B=\tfrac{1}{2}\Delta w,$$
$$\Delta=(E^A-E^B)/w,\qquad(26)$$

where Δ is the separation between atomic levels E^A and E^B, w is the valence band half width. It is convenient to use w as an energy unit throughout the calculation. Henceforth $w=1$ is assumed. Thus Δ represents the relative strength of the disorder in comparison to the periodic part of the Hamiltonian.

Unlike the case for metals, to evaluate the self-energy, Eq. (23), several additional features have to be addressed for a mixed semiconducting crystal with two basis atoms associated with each lattice point. First, the self-energy is now a 2×2 matrix because the two atoms in the unit cell introduce a bonding and an antibonding band. Second, if the near-neighbor interactions change with the atomic pairs then the concentration dependence of the $E_{\rm av}$ matrix is more involved. The formalism is now described in detail in the Appendix for the widely applicable zinc-blende structure which is appropriate for II-VI and III-V compound semiconductors.

For a two-band model of a semiconductor the Green's-function matrix is

$$\mathbf{G}(k,z)=\begin{bmatrix} z-s(k)-\Sigma_{aa}(z) & \Sigma_{ab}(z)\\ \Sigma_{ab}(z) & z+s(k)-\Sigma_{bb}(z)\end{bmatrix}^{-1},\qquad(27)$$

where $s(k)$ is the dispersion for the antibonding state (see the Appendix). In the case $\Sigma_{ab}(z)=0$, the CPA approach reduces to solving the following two decoupled equations self-consistently:

$$\Sigma_{aa}(z)=E_{aa}+\frac{c(1-c)\Delta_{aa}^2 f^{(0)}(z-\Sigma_{aa}-1)}{1+\{\Sigma_{aa}-E_{aa}-(1-2c)\Delta_{aa}\}f^{(0)}(z-\Sigma_{aa}-1)},\qquad(28)$$

$$\Sigma_{bb}(z)=E_{bb}+\frac{c(1-c)\Delta_{bb}^2 f^{(0)}(z-\Sigma_{bb}+1)}{1+\{\Sigma_{bb}-E_{bb}-(1-2c)\Delta_{bb}\}f^{(0)}(z-\Sigma_{bb}+1)},$$

$$f^{(0)}(z)\equiv\frac{1}{\pi}\int_{-\infty}^{\infty}\frac{d\eta\,\rho^{(0)}(\eta)}{z-\eta},\tag{29}$$

where

$$\rho^{(0)}(\eta)=\sum_k \delta[\eta-s(k)].$$

The averaged energies E_{ii}, and the energy separations between the host and impurity atoms for the bonding and antibonding bands Δ_{ii}, are defined as

$$E_{aa}=-(1-2c)\frac{\Delta}{2}+\frac{(1-c)E_g^B+cE_g^A}{2},$$
$$E_{bb}=-(1-2c)\frac{\Delta}{2}-\frac{(1-c)E_g^B+cE_g^A}{2},\tag{30}$$

$$\Delta_{aa}=\Delta+\frac{E_g^A-E_g^B}{2},$$
$$\Delta_{bb}=\Delta-\frac{E_g^A-E_g^B}{2}.\tag{31}$$

Note that unlike Eq. (26) for the single band case, the zero of energy is no longer set at the midpoint of either the antibonding states or the bonding states of the two pure crystals A and B.

The effects of alloying on electrons are contained in the self-energy functions $\Sigma(z)$. The real part of $\Sigma(z)$ in Eq. (28) represents the band shift and band distortion due to the disorder scattering. It is influenced by the entire region of the bands, whereas the imaginary part of $\Sigma(z)$ is determined by the lifetime of an electron at the energy z due to the disorder scattering.[29] In a non-self-consistent averaged t-matrix approximation (ATA), Equation (28) is solved when the $\Sigma(z)$ on the right-hand side of the equation is replaced by E_{ii}.

In the next section several contributions to the thermoelectric power in mixed crystals are obtained in detail.

IV. THERMOELECTRIC POWER IN MIXED CRYSTALS

In order to investigate the thermopower in mixed crystals the electrical conductivity σ in these systems is first examined because the off-diagonal transport coefficient $\sigma\alpha$ in Eq. (14) involves σ as a factor. The disorder induced electrical conductivity tensor in the CPA has been derived by Velicky.[8] In the mixed-crystal case, it has the form

$$\sigma=\frac{2e^2}{\pi\Omega}\int d\omega_2\left(-\frac{dn_f}{d\omega_2}\right)\times\int d\omega\sum_{n,k}[v_n(k)\mathrm{Im}\,G_{nn}(k,\omega_2)]^2\delta[\omega-E_n(k)].\tag{32}$$

For simplicity, only the diagonal part of the transport tensor is considered and the tensor subscripts are ignored in all following subsections. In Eq. (32) the summation over n includes the two bands under consideration, and the velocity is related to the energy dispersion $E_n(k)$ by $v_n(k)=\partial E_n(k)/\partial k$. The dispersion relations for the two bands of crystal B are $E_1(k)=s(k)$ and $E_2(k)=-s(k)$, respectively. When the tight-binding formalism, Eq. (A6), is used for the $s(k)$ of the diamond structure, the calculated σ curve displays structural details reflecting characteristics of the dispersion relation and does not affect the interpretation of the overall behavior of the thermopower. The configuration-averaged Green's functions in Eq. (32) for the two bands are obtained once the self-energies in Eq. (28) are determined by the self-consistent CPA approach. The summation over k in Eq. (32) may be performed using Monte Carlo sampling of $\frac{1}{48}$ of the Brillouzin zone.

It is known that electron-phonon mass enhancement affects the thermoelectric power. At low temperature, the scatterings of electrons by phonons and by impurities interfere with each other. Therefore the mass enhancement factors depend on the strength of the impurity scattering and the concentration of the impurities.

To obtain the thermoelectric power of a mixed crystal, Eqs. (10)–(13) are considered in the Bloch representation.

The thermoelectric power in a mixed crystal then can be expressed as the sum from three contributions:

$$\sigma\alpha=(\sigma\alpha)^{(1)}+(\sigma\alpha)^{(2)}+(\sigma\alpha)^{(3)}=\sum_s(\sigma\alpha)^{(s)}.\tag{33}$$

The first term $(\sigma\alpha)^{(1)}$ is the contribution from the part $j_e^E(\mathbf{r},t)-\mu j(\mathbf{r},t)$. The second and third terms come from the two electron-phonon interaction terms of $j_{ep}^E(\mathbf{r},t)$ in Eq. (11). They are related to the correlation functions in Eqs. (17) and (18), respectively.

The sum of the first two terms in Eq. (33) has special meaning. It is the so-called Mott term, $(\sigma\alpha)^{(M)}$, appearing in the Mott formula for metals.[6] It is related to the correlation function in Eq. (16) and, after performing the Matsubara sum, has the following form:

$$\begin{aligned}(\sigma\alpha)^{(M)}&=(\sigma\alpha)^{(1)}+(\sigma\alpha)^{(2)}\\&=\left(\frac{2\hbar}{\pi\Omega T}\right)\int_{-\infty}^{\infty}d\omega_2\left(-\frac{dn_f}{d\omega_2}\right)\omega_2\\&\quad\times\int d\omega\sum_{n,k}[v_n(k)\mathrm{Im}\,G_{nn}(k,\omega_2)]^2\\&\quad\times\delta[\omega-E_n(k)].\end{aligned}\tag{34}$$

The temperature dependence of $(\sigma\alpha)^{(M)}$ is implicitly contained in the Fermi distribution function n_f. The evaluation of Eq. (34) has the same degree of complexity as that of σ in Eq. (32). Thus by evaluating the $(\sigma\alpha)^{(M)}$, $(\sigma\alpha)^{(2)}$, and $(\sigma\alpha)^{(3)}$ separately, the relative importance of each contribution to the thermopower can be compared.

For $s=2$, 3 in Eq. (33), it is found

$$(\sigma\alpha)^{(s)}=\frac{1}{T\,d\hbar\,\Omega}\lim_{\omega\to 0}\mathrm{Im}\left(\frac{R^{(s)}(\omega+i\delta)}{\omega}\right),\tag{35}$$

where

$$R^{(2)}(i\omega)=\sum_{q\lambda} W_{\lambda}(q)\int_0^{\hbar\beta} d\tau\, e^{i\omega\tau}\langle T_\tau Q_\lambda(q,\tau)j(q,\tau)j(0)\rangle, \tag{36}$$

$$R^{(3)}(i\omega)=\sum_{q\lambda} \nabla_q W_{\lambda}(q) \times\int_0^{\hbar\beta} d\tau\, e^{i\omega\tau}\langle T_\tau \dot{Q}_\lambda(q,\tau)\rho(q,\tau)j(0)\rangle.$$

Consider the lattice Fourier transform of Eq. (20). Define the following configuration averages of the phonon Green's function and the electron density-density correlation function

$$D(q,\tau)\equiv-\langle T_\tau[a_{q\lambda}(\tau)+a^+_{-q\lambda}(\tau)][a_{-q\lambda}(0)+a^+_{q\lambda}(0)]\rangle, \tag{37}$$

$$S(q,\tau)\equiv-\langle T_\tau\rho(q,\tau)\rho(-q,0)\rangle. \tag{38}$$

Carrying out the Matsubara sums in Eq. (36), the following expressions are obtained:

$$(\sigma\alpha)^{(2)}=\frac{1}{T\,d\Omega\,\hbar}\sum_{q\lambda}\frac{|M_\lambda(q)|^2}{m}\int_{-\infty}^{\infty}\frac{d\omega_2}{2\pi}\omega_2\,\mathrm{Im}\,S(q,\omega_2) \times\left[\frac{\partial^2 n_B}{\partial\omega_2^2}\mathrm{Im}\,D(q,\omega_2)+2\left(\frac{\partial n_B}{\partial\omega_2}\right)\left(\frac{\partial\,\mathrm{Im}\,D(q,\omega_2)}{\partial\omega_2}\right)\right], \tag{39}$$

$$(\sigma\alpha)^{(3)}=\frac{1}{T\,d\Omega\,\hbar}\sum_{q\lambda}\frac{q\cdot\nabla_q(\omega_q|M_\lambda(q)|^2)}{m\omega_q} \times\int_{-\infty}^{\infty}\frac{d\omega_2}{2\pi}\omega_2\,\mathrm{Im}\,D_\lambda(q,\omega_2) \times\left[\frac{\partial^2 n_B}{\partial\omega_2^2}\mathrm{Im}\,S(q,\omega_2)+2\left(\frac{\partial n_B}{\partial\omega_2}\right)\left(\frac{\partial\,\mathrm{Im}\,S(q,\omega_2)}{\partial\omega_2}\right)\right]. \tag{40}$$

Here n_B represents the Boson distribution function and the conventional notation for electron-phonon matrix element, instead of $W_\lambda(q)$, is used:

$$M_\lambda(q)\equiv W_\lambda(q)\left(\frac{\hbar}{2M\omega_{q\lambda}}\right)^{1/2}. \tag{41}$$

Equations (39) and (40) are general expressions for the contribution of electron-phonon interaction to the thermopower in terms of the phonon Green's function and the electron density-density correlation function for any system. For pure metals they reduce to the expressions given in JM.

The calculation of $(\sigma\alpha)^{(2)}$ and $(\sigma\alpha)^{(3)}$ in Eqs. (39) and (40) for disordered mixed crystals now involves three parts: (i) the determination of the configuration averages of the electron density-density correlation function $S(q,\omega)$, (ii) the determination of the dielectric functions in mixed semiconductors, and (iii) the determination of phonon Green's function $D(q,\omega)$ for a disordered crystal.

A. Averaged density-density correlation function

The density-density correlation function $S(q,i\omega)$ in Eq. (38) is related to the electron propagation propagator $P(q,i\omega)$ in the following way:

$$S(q,i\omega)=\frac{-P(q,i\omega)}{\varepsilon(q)} =\frac{-1}{\varepsilon(q)}\sum_j\sum_{is}\int\frac{d^3k_1}{(2\pi)^3} \times G^j(k_1+q;\ is+i\omega)G^j(k_1;is). \tag{42}$$

Here $G^j(k_1;\ \text{is})$ represents the electron Green's function associated with the jth band, and $\varepsilon(q)$ the wave-number-dependent dielectric function.

$$\text{Therefore}\quad \mathrm{Im}\,S(q,i\omega)=\frac{\mathrm{Im}\,P(q,i\omega)}{\varepsilon(q)^2} \tag{43}$$

and after Matsubara summation in Eq. (42), we have

$$\mathrm{Im}\,P(q,\omega+i\delta)=\omega\sum_j\int\frac{d^3k_1}{(2\pi)^3}\int_{-\infty}^{\infty}\left(\frac{d\omega_2}{2\pi}\right) \times G^j_{k_1+q}(\omega+\omega_2)G^j_{k_1}(\omega_2)\frac{\partial n_F}{\partial\omega_2}; \tag{44}$$

here the configuration averaged Green's function is defined in Eq. (27) in terms of the self-energy in the mixed crystal.

B. Dielectric function for the mixed crystal

The static dielectric constants of semiconductors are known to be much larger than 1. The wave-number-dependent dielectric function $\varepsilon(q)$ for a semiconductor is different from that of the free-electron gas because of the importance of contributions from Bragg reflections and Umklapp processes. Penn[12] used an isotropic energy-band model allowing for the possibility of Umklapp processes to derive the wave-number-dependent dielectric function for semiconductors. Reasonable $\varepsilon(q)$ for small values of q were obtained. Nara[13] later used realistic band structures and oscillator strengths to calculate the $\varepsilon(q)$ and confirmed that anisotropic effects and the off-diagonal matrix elements of the dielectric tensors $\varepsilon(q+K,q+K')$ with reciprocal lattice vectors K not equal to K' are indeed small. The averaged dielectric function for the mixed crystal are then derived based on the assumptions

$$\varepsilon(q)=c\varepsilon^A(q)+(1-c)\varepsilon^B(q), \tag{45}$$

$$(k_F)^3=c(k_F^A)^3+(1-c)(k_F^B)^3. \tag{46}$$

k_F is the Fermi momentum of the mixed crystal.

With the dielectric function and the self-energy of the mixed crystal determined, the correlation function $\mathrm{Im}\,S(q)$ in Eq. (43) for the mixed semiconductor is readily evaluated.

C. Averaged phonon Green's functions

The configuration-averaged phonon Green's function in Eqs. (39) and (40) used in this work are derived from Flicker and Leath's work.[10] One obtains

$$\langle D_\lambda(q,\omega,i\delta)\rangle_{\mathrm{av}}=\frac{2(1-c)\omega_{q\lambda}}{(\omega^2-\omega_{q\lambda}^2)+2i\delta\omega}+\frac{2c\gamma b_{q\lambda}}{(\omega^2-b_{q\lambda}^2)+2i\delta\omega}. \tag{47}$$

$\omega_{q\lambda}$ is the phonon frequency corresponding to the λth branch and momentum q, and

$$b_{q\lambda}\equiv\sqrt{\frac{M_B}{M_A}}\,\omega_{q\lambda}\equiv\gamma\omega_{q\lambda}. \tag{48}$$

M_B and M_A are the mass of atoms B and A, respectively. Thus

$$\langle \mathrm{Im}\,D_\lambda(q,\omega+i\delta)\rangle_{\mathrm{av}}=(1-c)\pi\omega_{q\lambda}\delta(\omega^2-\omega_{q\lambda}^2)+c\pi\gamma b_{q\lambda}\delta(\omega^2-b_{q\lambda}^2). \tag{49}$$

From the above expression for the configuration-averaged phonon Green's function, the off-diagonal transport coefficient in Eqs. (39) and (40) for the mixed crystal becomes

$$\begin{aligned}(\sigma\alpha)^{(2)}=&\sum_{q\lambda}A_{q\lambda}^{(2)}(1-c)\Bigg[\Bigg\{\mathrm{Im}\,S(q,\omega_{q\lambda})\\&+\omega_{q\lambda}\frac{\partial\,\mathrm{Im}\,S(q,\omega_{q\lambda})}{\partial\omega_{q\lambda}}\Bigg\}\frac{\partial n_B}{\partial\omega_{q\lambda}}\\&+\frac{\omega_{q\lambda}\,\mathrm{Im}\,S(q,\omega_{q\lambda})}{2}\left(\frac{\partial^2 n_B}{\partial\omega_{q\lambda}^2}\right)\Bigg]\\&+\sum_{q\lambda}A_{q\lambda}^{(2)}c\gamma\Bigg[\Bigg\{\mathrm{Im}\,S(q,b_{q\lambda})\\&+b_{q\lambda}\frac{\partial\,\mathrm{Im}\,S(q,b_{q\lambda})}{\partial b_{q\lambda}}\Bigg\}\frac{\partial n_B}{\partial b_{q\lambda}}\\&+\frac{b_{q\lambda}\,\mathrm{Im}\,S(q,b_{q\lambda})}{2}\left(\frac{\partial^2 n_B}{\partial b_{q\lambda}^2}\right)\Bigg],\end{aligned} \tag{50}$$

where

$$A_{q\lambda}^{(2)}=\left(\frac{2}{T\hbar\,d\Omega}\right)\left(\frac{|M_\lambda(q)|^2}{m}\right)$$

$$\begin{aligned}(\sigma\alpha)^{(3)}=&\sum_{q\lambda}A_{q\lambda}^{(3)}(1-c)\Bigg[\Bigg\{\omega_{q\lambda}\frac{\partial\,\mathrm{Im}\,S(q,\omega_{q\lambda})}{\partial\omega_{q\lambda}}\Bigg\}\frac{\partial n_B}{\partial\omega_{q\lambda}}\\&+\frac{\omega_{q\lambda}\,\mathrm{Im}\,S(q,\omega_{q\lambda})}{2}\left(\frac{\partial^2 n_B}{\partial\omega_{q\lambda}^2}\right)\Bigg]\\&+\sum_{q\lambda}A_{q\lambda}^{(3)}c\gamma\Bigg[\Bigg\{b_{q\lambda}\frac{\partial\,\mathrm{Im}\,S(q,b_{q\lambda})}{\partial b_{q\lambda}}\Bigg\}\frac{\partial n_B}{\partial b_{q\lambda}}\\&+\frac{b_{q\lambda}\,\mathrm{Im}\,S(q,b_{q\lambda})}{2}\left(\frac{\partial^2 n_B}{\partial b_{q\lambda}^2}\right)\Bigg],\end{aligned} \tag{51}$$

where

$$A_{q\lambda}^{(3)}=\left(\frac{2}{T\hbar\,d\Omega}\right)\left(\frac{q\cdot\nabla_q(\omega_{q\lambda}|M_\lambda(q)|^2)}{\omega_{q\lambda}}\right).$$

In the next section, numerical results for only the parts of the thermopower of Si-Ge system given by Eqs. (34), (50), and (51) are presented. In addition, the validity of ATA and CPA approximations for several values of c is assessed for this system.

V. NUMERICAL RESULTS FOR Si_{1-c}-Ge_c MIXED CRYSTALS

As an illustration of the formalism developed here for the thermoelectric transport parameters for disordered mixed semiconductors, the Si_{1-c}-Ge_c system is now considered. The band parameters used are $\Delta=0.816$, $E_g^B=1.2\,\mathrm{eV}$, $E_g^A=0.7\,\mathrm{eV}$. The calculation of the transport coefficients in the thermoelectric matrix was performed only at the room temperature and for a few values of c. The choice of the room temperature in our calculation allows us to make zero-temperature approximations in view of the energetics of the bands concerned. The experimental results are reported as a function of temperature but for limited values of filling of the bands for several c's. We perform theoretical calculations at room temperature but for few values of c to keep the computation within reasonable limits. The change of dielectric functions in the mixed semiconductors, and the existence of two bands are taken into account in this calculation.

A. Concentration dependence of the self-energy

To assess the validity of the ATA and CPA, the self-energies in both schemes are calculated for the two bands using Eq. (28). The results are displayed in Fig. 1 for $c=0.4$. Unlike the case of metallic Ag-Au alloys,[11] the deviation between the two approximations is quite significant for this concentration. Not only the shapes of the real and imaginary parts of the self-energies are different, but also the extents of those energies are different. This is in contrast to the Ag-Au system considered before[11] because the constituent d subbands lie within the broad s bands of this metallic alloy, whereas the two subbands in Si-Ge under consideration do not overlap. This result is of particular importance since the ATA may be regarded as a good approximation for metallic alloys, but the CPA self-consistent approach appears to be crucial in getting a reliable result for the semiconductor case.

To obtain the c dependence of the self-energies, the computations for $c=0.1$ (Fig. 2) and $c=0.4$ are compared. It is observed that the varying part of the real $\Sigma(z)$ is more extended in energy as c increases. For energies $z<-3$ and $z>+3$, the real parts of $\Sigma(z)$ approach some constants for both the bonding and antibonding bands. These constants increase with the impurity concentration c representing the changes of band edges with c. Alloy disorder is found to have relatively weaker effects near the forbidden energy gaps. Away from the gap, the self-energy is more severely affected by alloying as can be seen by comparing Figs. 1 and 2.

The imaginary part of $\Sigma(z)$ for $c=0.1$ (Fig. 2) is smaller for the lower part of the bands and greater near the top of the bands indicating that states near the top of the bands are

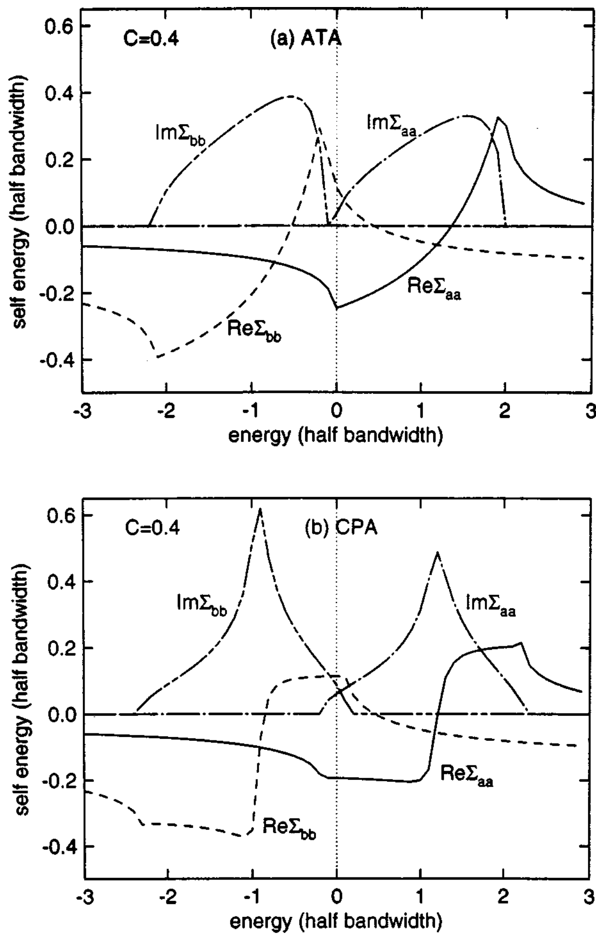

FIG. 1. The real part and imaginary part of the self-energies for the bonding and antibonding bands for Si_{1-c}-Ge_c with $c=0.4$ calculated using (a) ATA and (b) self-consistent CPA.

preferentially damped by the presence of the impurities. However, as c increases, this preferential damping moves to lower part of the bands and the corresponding damping also increases (see Fig. 1). Alternatively, the $\mathrm{Im}\,\Sigma=\Gamma$ in Fig. 2 can be understood as follows. Each of the bonding and the antibonding bands now contains two overlaping subbands; the host subband and the impurity subband. The peak of Γ is in the impurity subband region and the low-energy tail part of Γ is in the host subband region. Both the bandwidth and the height of the impurity subband increase with concentration. Therefore for $c=0.4$, as shown in Fig. 1, Γ approaches a symmetric shape characteristic of the merging of the two subbands.

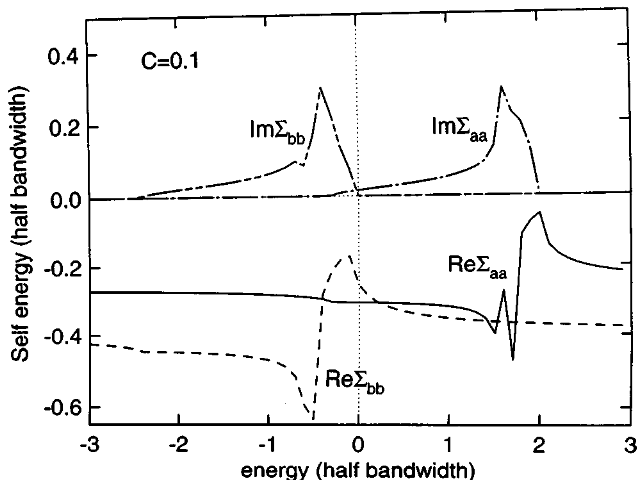

FIG. 2. The real part and imaginary part of the self-energies for the bonding and antibonding bands for Si_{1-c}-Ge_c with $c=0.1$ calculated using self-consistent CPA.

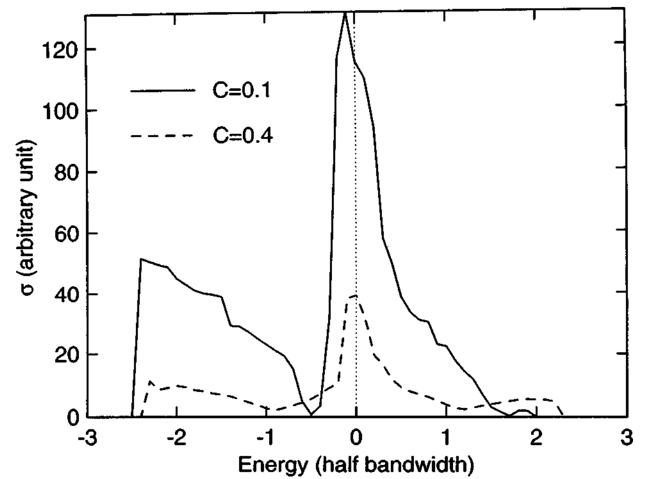

FIG. 3. The electrical conductivity σ as a function of the chemical potential (filling of the bands) for disordered Si_{1-c}-Ge_c with $c=0.4$ (dashed curve) and $c=0.1$ (solid curve).

B. Disorder contribution to σ

The integration over k_l in Eq. (44) is done using Monte Carlo sampling of 2000 random points in $\frac{1}{48}$th of the Brillouin zone of the diamond structure given by $k_z<k_y<k_x<1$, $k_x+k_y+k_z<\frac{3}{2}$. It is found that for the room-temperature case $\partial n_F/\partial\omega_2$ is very close to a delta function at the chemical potential μ. The calculated disorder scattering contribution to the static electrical conductivity in Eq. (32) is given in Fig. 3 as a function of the filling of the two bands for two concentrations $c=0.1$ and $c=0.4$. This is equivalent to investigating dependence on doping density. The maxima of the conductivity occur near the bottom of both the bonding and antibonding bands. These maxima reduce in intensity as c increases toward $c=0.5$ and increase in intensity again for higher c, as a result of stronger multiple impurity scatterings occuring at the intermediate concentration range and causing a reduction of the electrical conductivity. The shape of the σ curve may be understood as follows. At small occupation numbers of the band, the Fermi level is located in the host band and the carriers move mostly between the host atoms, having a high mobility. When the occupation number increases, the Fermi level approaches the impurity band and more carriers are energetically found in the impurity band region and their mobility is thus reduced. Thus we see the asymmetry of the σ curve in the bonding and antibonding band regions. Also to be noted is that for higher concentration c, the impurity subband plays a relatively more important role. As shown in Fig. 3, the distinguishing contribution from impurity subbands for $c=0.4$ produces shoulder structures in the energy ranges $1<E<2.5$ and $-1<E<0$, where the impurity subbands are located, whereas these shoulders are absent for $c=0.1$.

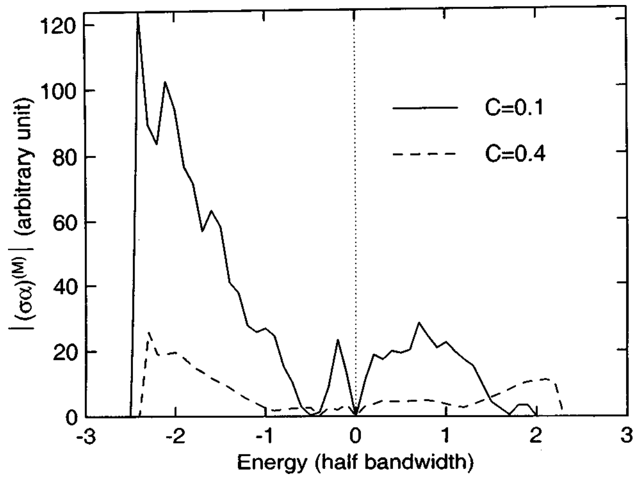

FIG. 4. The absolute value of thermopower $|(\sigma\alpha)^{(M)}|$ as a function of the chemical potential (filling of the bands) for disordered Si_{1-c}-Ge_c with $c=0.4$ (dashed curve) and $c=0.1$ (solid curve).

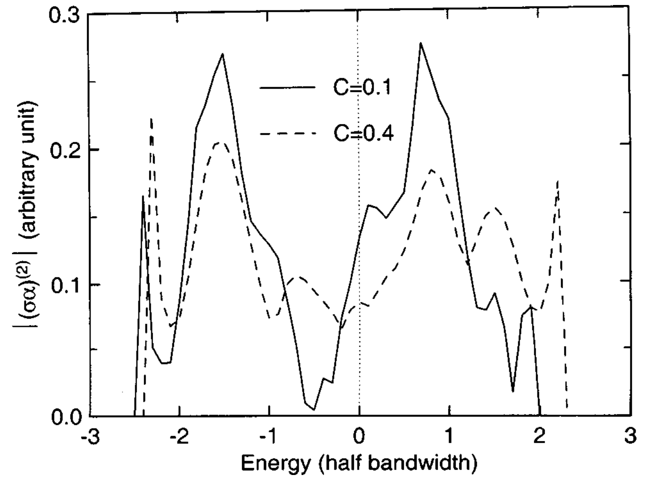

FIG. 5. The absolute value of thermopower $|(\sigma\alpha)^{(2)}|$ as a function of the chemical potential (filling of the bands) for disordered Si_{1-c}-Ge_c with $c=0.4$ (dashed curve) and $c=0.1$ (solid curve).

We also calculate the effects of energy gap E_g^B and relative strength of disorder Δ on the conductivity σ. The increase of the gap and Δ does not alter the shape of the conductivity curve. The change in the shape of the curve is insignificant. The increase of the strength of disorder Δ has two effects. It moves the gap to lower energies and it lowers the conductivity. For negative values of Δ, that is, for the host atoms having higher atomic level than the impurity atoms, we have $\sigma(E,-\Delta)=\sigma(-E,\Delta)$.

C. Dependences of $(\sigma\alpha)^{(M)}$, $(\sigma\alpha)^{(2)}$, and $(\sigma\alpha)^{(3)}$ on c and band filling

The dielectric functions for pure Si and Ge given by Srinivasan[14] employing Penn's model for an extended range of q are used. Equation (45) is then used to obtain the averaged dielectric function for the evaluation of the density-density correlation functions in Eq. (43). In Fig. 4, for ease of presentation, the calculated results of the absolute value of $(\sigma\alpha)^{(M)}$ due to disorder scattering for $c=0.1$ and 0.4 are displayed as a function of the filling of the two bands as in Fig. 3. Note that this representation does not display explicitly the change in a sign of $(\sigma\alpha)^{(M)}$ in some regions of energy in Fig. 4. It is interesting to note that their dependence on the occupancy of bands is quite different from that of the static electrical conductivity in Fig. 3. The $|(\sigma\alpha)^{(M)}|$ for holes is greater than for electrons. Again, like σ, it decreases with concentration c.

The calculated absolute magnitude $|(\sigma\alpha)^{(2)}|$ in Eq. (50) for the disordered Si_{1-c}-Ge_c is similarly shown in Fig. 5 for $c=0.1$ and $c=0.4$. Since this quantity is related to the electron-phonon coupling, its dependence of the filling of the bands is quite symmetric in contrast to the corresponding σ or $|(\sigma\alpha)^{(M)}|$ curve. It follows more or less the shape of the host crystal electron density of states for low impurity concentrations. For $c=0.4$, the impurity subbands produce prominent structures in the regions $1<E<2.5$ and $-1<E<0$ similar to that for σ. But instead of shoulders, new peaks appear. The increase of the strength of disorder for $c=0.1$ moves the curve to lower energy in a similar manner as for the case of σ.

Vilenkin and Taylor[23] were the first to derive the term $(\sigma\alpha)^{(3)}$ coming from the contribution of phonon momentum and they neglected it as small in comparison to $(\sigma\alpha)^{(2)}$. Furthermore, Jonson and Mahan[6] found that it is negligible at both high and low temperatures for a metal. Here we find the calculated absolute value of $(\sigma\alpha)^{(3)}$ in Eq. (51), which is related to the term with phonon momentum, is about an order of magnitude smaller than that of $|(\sigma\alpha)^{(2)}|$ for semiconductors but is not entirely negligible at room temperature. As shown in Fig. 6, the impurity subbands again produce structures for $c=0.4$ similar to the case of $|(\sigma\alpha)^{(2)}|$.

D. Discussion of the numerical results

In general, because of the charge transfer between the two bands for a mixed crystal, the transport coefficients near the band gaps are different from those from the single band approach. This becomes most important for higher alloy concentrations.

In semiconducting alloy systems there are four prominent electron-scattering mechanisms with different relative

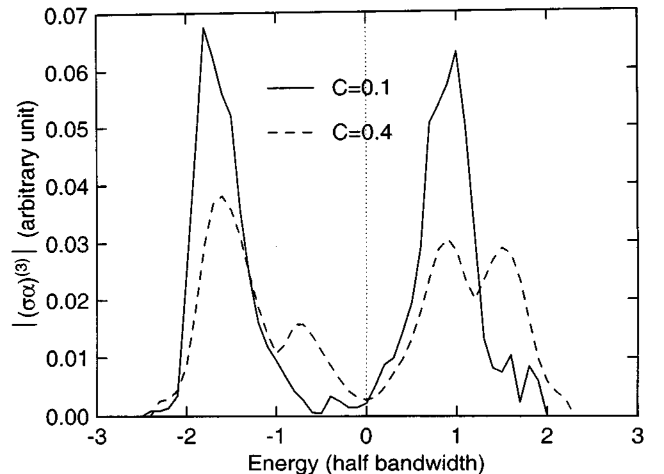

FIG. 6. The absolute value of thermopower $|(\sigma\alpha)^{(3)}|$ as a function of the chemical potential (filling of the bands) for disordered Si_{1-c}-Ge_c with $c=0.4$ (dashed curve) and $c=0.1$ (solid curve).

weights at different situations: the scattering by acoustical phonons, alloy disorder, ionized impurities, and the intervalley scattering. Amith[30] made measurements of the Seebeck coefficients in the ''competitive'' region and analyzed the data based on the relative importance of these mechanisms. The conclusion is that a qualitative interpretation is obtained only when all the mechanisms are invoked.

Experimental measurements of the thermoelectric transport coefficients in the Si-Ge systems as a function of temperature and for a limited number of doping densities and composition c have been reported previously.[30–35] The thermal resistivity as a function of composition c was found to have a broad maximum near the middle of the alloy composition.[31,32] However, for power generation applications at high temperatures, a high melting point and a large band gap are also important, favoring the Si-rich alloys. Dismukes *et al.*[31] measured the thermoelectric transport coefficients for several Si-rich n-type and p-type alloys as functions of carrier concentration and temperature. They found that at 300 K and for constant carrier concentration the Seebeck coefficient α and the electrical resistivity ρ increases only slightly with increasing Si content in the range $c<0.4$, while for $c=0.8$ the α is about 23% smaller than that for $c=0.3$ in the Si_{1-c}-Ge_c system presumably due to the change of number of valleys in the band structures for higher Ge content.[30,31] The dependences of α and ρ on carrier concentration and temperature are very pronounced. For a given temperature, α and ρ decrease when the carrier concentration increases. On the other hand, for given carrier concentration, the α and ρ increase with temperature. Additional features are observed for n-type alloys at high temperature. The α and ρ for n-type alloys reach maxima and then decrease with temperature possibly due to the onset of intrinsic conduction.

For heavily doped n-type and p-type Si and Ge crystals Fistul'[36] measured the α and ρ as functions of carrier concentration and temperature. He found that within the limits of the experimental error the value of α at room temperature does not depend upon the chemical nature of the dopants and the phonon drag is negligible. Similar measurements were also done for samples of different carrier concentrations by other authors.[37,38] In the next paragraph, a discussion of the electron-phonon contribution will be shown to be an order of magnitude smaller.

These two sets of measurement lead naturally to our estimation of the difference of the results between the pure and the mixed crystals with the same carrier concentration. This gives the disorder contribution to the α which may be compared with the calculations of this work. For $c=0.3$ and $n=2.2\times10^{18}$/c.c. case,[31,37] the difference is 220 μV/K; for $n=6\times10^{19}$/c.c. case[31,38] it is 130 μV/K. The disorder contributions to the Mott term are calculated to be $\alpha^{(M)}=120\,\mu$V/K and 130 μV/K, respectively, for these two concentrations. The agreement is fairly good in view of the uncertainty in assuming that the same relationship between chemical potential and carrier concentration holds for both pure Si and the mixed-crystal system. In the next paragraph, a discussion of the electron-phonon contribution will be shown to be an order of magnitude smaller.

For Si-Ge mixed crystals the phonon mean free paths are short, and therefore, unlike pure Si or Ge, the phonon drag contributions are negligible in comparison with the electronic part. In this work we calculated only the electron-phonon contribution to the electronic part of the thermopower of a mixed semiconductor. The intervalley scattering, ionized-impurity scattering for heavily doped alloys were not included. For comparison with the measured transport coefficients of Si-Ge mixed crystal with $c=0.3$ in Ref. 31, the calculations presented here give $|(\sigma\alpha)^{(2)}|=2116\,(\Omega\text{ cm deg})^{-1}\,\mu$V, and $|(\sigma\alpha)^{(3)}|=132.7\,(\Omega\text{ cm deg})^{-1}\,\mu$V. The measured $(\sigma\alpha)$, on the other hand, at $n=2.2\times10^{19}$/c.c. is 26670 $(\Omega\text{ cm deg})^{-1}\,\mu$V. Thus the present calculated disorder contribution to $(\sigma\alpha)^{(2)}$ is an order of magnitude smaller and $(\sigma\alpha)^{(3)}$ is two orders of magnitude smaller than the measured $(\sigma\alpha)$. It is safe to conclude that the electron-phonon interaction in this disordered system with $c=0.3$ contributes only 10% of the total $(\sigma\alpha)$.

To measure the quality of materials for thermoelectric device applications one defines a figure of merit ZT in terms of several transport coefficients appearing in Eq. (14):

$$ZT=\frac{\sigma\alpha^2T}{\kappa}. \tag{52}$$

Sofo and Mahan[39] analyzed the optimum band gap of a thermoelectric material with best performance. The optimum band gap at operating temperature T was found by them to be $10k_BT$. The Si-Ge systems have band gaps that obey this rule for better thermoelectric materials at operating temperature around 1000 K. Measurements as well as model calculations for lattice thermal conductivity in the Si-Ge alloy systems have been very extensive. Theoretical model calculations using the relaxation time approximation all indicate that the lattice thermal conductivity of the Si-Ge mixed crystals is an order of magnitude lower than the parent pure crystals and decreases with increasing temperature.[40–42] Because the carrier mobility is only slightly smaller in the mixed crystal than in the pure crystals, the estimated thermoelectric figure of merit of the mixed crystals can reach $ZT=0.8$ for $c=0.3$ at 1000 K using the experimental measured values of transport coefficients[31] in Eq. (52), while the estimated ZT is ≈0.1 at 300 K. The maximum figure of merit above 1000 K, on the other hand, has been estimated to be $ZT\approx1.13$.[41] The present calculation at room temperature shows that the thermopower from disorder effect in the normal carrier concentration range is 30–45% less than that of the pure Si, which confirms that the increase of ZT from Eq. (52) in this disordered system may arise mainly from the disorder effect on the thermal conductivity.

VI. SUMMARY

In this contribution, an expression for the energy–current-density is given in a general setting which unifies the results found in the literature in an elegant way. The general density-density correlation function which describes semiconductors is considered here which is different from the case of metals often treated in the literature. This formulation also incorporates coherent potential approximations useful in dealing with disordered mixed crystals as well as electron-phonon interactions. In metals, Jonson and Mahan[6] found that the nonadiabatic part of electron-ion contributions is negligible so that Mott's formula for thermoelectric power

continues to hold. In the case of strongly coupled electron-ion systems which may occur in semiconductors, this conclusion needs to be examined. Here it is found that the frequently omitted term is one order of magnitude smaller than the Mott term, but not entirely negligible.

The electronic, adiabatic electron-phonon, and nonadiabatic electron-phonon contributions to the thermoelectric power in disordered mixed crystals using multiband CPA are derived in this work. Only the disorder contributions to the thermopower and electrical conductivity in mixed Si-Ge crystals are investigated as an illustration of the formalism given here. Here the Wannier/Bloch representation is used to describe the system under consideration. The nonparabolicity of the bands with band gap and the semiconductor dielectric functions are included to give a realistic description of the semiconducting system. The results for this system show that the disorder effect does not introduce significant change in the electrical conductivity but indicates a decrease in its thermopower. Therefore it is the dramatic reduction in the thermal conductivity of disordered systems that raises the thermoelectric figure of merit. Since the calculated concentration and band occupancy dependences of the diagonal and off-diagonal transport coefficients are different, one may also use these dependences to tailor the maximum value of thermoelectric figure of merit in a mixed crystal. The formalism presented here for the thermopower in disordered crystals is quite general and may be used in the study of other semiconducting systems.

ACKNOWLEDGMENTS

This work was supported in part by the Office of Naval Research. A.K.R. thanks Professor S. D. Mahanti for several discussions on the contents of this paper.

APPENDIX

In this Appendix, we give the salient features of the electronic structure of a model semiconductor with the two basis atoms $i=1$, 2 associated with each lattice point n of a zincblend lattice. (These two basis atoms are identical for group-IV materials.) This model is used in the calculations presented in this paper. The Hamiltonian of this system in the Wannier representation is

$$H=\sum_{n,i} |n,i\rangle\varepsilon_n^i(x)\langle n,i| + \sum_{\substack{n,n',i,j\\ ni\neq n'j}} |n,i\rangle V_{ij}(\mathbf{r}_{ni}-\mathbf{r}_{n'j})\langle n',j|. \tag{A1}$$

$|n,i\rangle$ represents the Wannier state associated with the nth lattice point of the ith sublattice. The diagonal term $\varepsilon_n^i(x)$ depends upon whether the site n,i is occupied by the host atom or the impurity atom ($x=$atom$B$ or A).

In general, in CPA the V_{12} is considered to be independent of the impurity concentration c as it only appears in the dispersive part of the Hamiltonian for the metals. In the present case for semiconductors, V_{12} appears both in the dispersive and nondispersive parts. The latter determines the splitting of the bonding and antibonding states and the former determines the dispersion of the bonding band and antibonding bands. The c dependence of V_{12} is included in the latter and ignored in the former part. It may be estimated through a mean field seen by an atom when the impurity is present

$$\langle V_{12}\rangle=(1-c)V_{B-B}+cV_{A-A}. \tag{A2}$$

A simplified approach can be developed when only nearest-neighbor interactions are considered. Then the following substitutions representing the antibonding and bonding states are made:

$$|n,a\rangle=\frac{1}{\sqrt{2}}[|n,1\rangle+|n,2\rangle],$$
$$|n,b\rangle=\frac{1}{\sqrt{2}}[|n,1\rangle-|n,2\rangle], \tag{A3}$$

so that Eq. (A1) can be rewritten in the following simpler form:

$$H=\sum_n |n,a\rangle(\varepsilon_n^{(a)}(x))\langle n,a|+\sum_n |n,b\rangle(\varepsilon_n^{(b)}(x))\langle n,b| + \frac{1}{2}\sum_{n\neq n'} [|n,a\rangle V_{12}\langle n',a|-|n,b\rangle V_{12}\langle n',b|], \tag{A4}$$

where

$$\varepsilon_n^{(a)}\equiv\tfrac{1}{2}(\varepsilon_n^{(1)}+\varepsilon_n^{(2)}+V_{12}),$$
$$\varepsilon_n^{(b)}\equiv\tfrac{1}{2}(\varepsilon_n^{(1)}+\varepsilon_n^{(2)}-V_{12}). \tag{A5}$$

$\varepsilon_n^{(a)}$ and $\varepsilon_n^{(b)}$ represent the energies for the antibonding and bonding states at the center of the Brillouin zone, respectively. The last summation in Eq. (A4) is the dispersion for the bonding and antibonding states. For example, for the diamond lattice the dispersion relation for the antibonding state can be expressed, in units of half bandwidth w as

$$s(k)=\left[\cos^2\frac{\pi k_x}{2}\cos^2\frac{\pi k_y}{2}\cos^2\frac{\pi k_z}{2} + \sin^2\frac{\pi k_x}{2}\sin^2\frac{\pi k_y}{2}\sin^2\frac{\pi k_z}{2}\right]^{1/2}. \tag{A6}$$

For the bonding band the dispersion relation is $-s(k)$.

Using the Hamiltonian in Eq. (A4) we obtain the two-band Green's-function matrix given in Eq. (27). At this stage it is convenient to use a model density of states $\rho^{(0)}(\eta)$ to obtain an analytical solution of the integral in Eq. (29). Let

$$\rho^{(0)}(E)=\begin{cases}\left(\frac{1}{\pi}\right)\left[1-\left(E-1-\frac{E_g}{2}\right)^2\right]^{1/2}; & \left|E-1-\frac{E_g}{2}\right|\leqslant 1\\ \left(\frac{1}{\pi}\right)\left[1-\left(E+1+\frac{E_g}{2}\right)^2\right]^{1/2}; & \left|E+1+\frac{E_g}{2}\right|\leqslant 1\\ 0 & \text{elsewhere.}\end{cases} \tag{A7}$$

Here and elsewhere, the energy units are in terms of the half bandwidth. This density of states has no critical point except at the band edges.

This model density of states produces an analytical form of the electron Green's function for the pure semiconductors. The analytical solution of the integral in Eq. (29) using complex variables is found to be

$$f^{(0)}(z)=2\left\{x\left(1-B\cos\frac{A}{2}\theta_{>}\right)+yB\sin\frac{A}{2}\theta_{>}+|z|B\sin\frac{A}{2}\theta_{<}\right\}+2i\left\{y\left(1-B\cos\frac{A}{2}\theta_{>}\right)-xB\sin\frac{A}{2}\theta_{>}-|z|B\cos\frac{A}{2}\theta_{<}\right\} \tag{A8}$$

for $z=x+iy$, and

$$A\equiv\tan^{-1}\frac{2xy}{x^2-y^2-1};\quad B\equiv\frac{[(x^2-y^2-1)^2+4x^2y^2]^{1/4}}{(x^2+y^2)^{1/2}}, \tag{A9}$$

$$\theta_{<}=1\quad\text{when}\ \operatorname{Re}z^2<1,\ \text{and}\ \theta_{<}=0\quad\text{otherwise,}$$

$$\theta_{>}=1\quad\text{when}\ \operatorname{Re}z^2>1,\ \text{and}\ \theta_{>}=0\quad\text{otherwise.} \tag{A10}$$

These analytical results are used in the computations discussed in the paper.

[1] P. J. Lin-Chung and A. K. Rajagopal, *Proceedings of the 15th International Conference on Thermoelectrics* (IEEE Inc., Piscataway, NJ, 1996), p. 209.
[2] R. Kubo, J. Phys. Soc. Jpn. **12**, 570 (1957).
[3] R. Kubo, M. Yokota, and S. Nakajima, J. Phys. Soc. Jpn. **12**, 1203 (1957).
[4] L. P. Kandanoff and P. C. Martin, Phys. Rev. **124**, 670 (1961).
[5] J. M. Luttinger, Phys. Rev. **135**, A1505 (1964).
[6] M. Jonson and G. D. Mahan, Phys. Rev. B **21**, 4223 (1980); **42**, 9350 (1990).
[7] A. Ourmazd, D. W. Taylor, J. Cunningham, and C. W. Tu, Phys. Rev. Lett. **62**, 933 (1989); D. Gammon, E. S. Snow, B. V. Shanabrook, D. S. Katzer, and D. Park, *ibid.* **76**, 3005 (1996).
[8] B. Velicky, Phys. Rev. **184**, 614 (1969).
[9] R. J. Elliott, J. A. Krumhansl, and P. L. Leath, Rev. Mod. Phys. **46**, 465 (1974).
[10] J. K. Flicker and P. L. Leath, Phys. Rev. B **7**, 2296 (1973).
[11] L. Schwartz, F. Brouers, A. V. Vedyayev, and H. Ehrenreich, Phys. Rev. B **4**, 3383 (1971).
[12] D. R. Penn, Phys. Rev. **128**, 2093 (1962).
[13] H. Nara, J. Phys. Soc. Jpn. **20**, 778 (1965); **20**, 1097 (1965).
[14] G. Srinivasan, Phys. Rev. **178**, 1244 (1969).
[15] A. Yamamoto and T. Ohta, *Proceedings of the 15th International Conference on Thermoelectrics* (Ref. 1), p. 464.
[16] X. Z. Sun, M. S. Dresselhaus, G. Chen, and K. L. Wang, Bull. Am. Phys. Soc. **43**, 461 (1998).
[17] D. Stroud and H. Ehrenreich, Phys. Rev. B **2**, 3197 (1970).
[18] J. E. Bernard and A. Zunger, Phys. Rev. B **44**, 1663 (1991).
[19] G. Theodorou, P. C. Kelires, and C. Tserbak, Phys. Rev. B **50**, 18 355 (1994).
[20] See, for example, B. R. Nag, *Electron Transport in Compound Semiconductors* (Springer-Verlag, New York, 1980), Chap. 8.
[21] R. J. Hardy, Phys. Rev. **132**, 168 (1963).
[22] S. K. Lyo, Phys. Rev. B **17**, 2545 (1978).
[23] A. Vilenkin and P. L. Taylor, Phys. Rev. B **18**, 5280 (1978).
[24] L. Friedman, J. Phys. C **17**, 3999 (1984).
[25] K. Durczewski and M. Ausloos, Phys. Rev. B **53**, 1762 (1996).
[26] B. Velicky, S. Kirkpatrick, and H. Ehrenreich, Phys. Rev. **175**, 747 (1968).
[27] P. Soven, Phys. Rev. **156**, 809 (1967).
[28] D. W. Taylor, Phys. Rev. **156**, 1017 (1967).
[29] H. Ehrenreich and K. C. Hass, J. Vac. Sci. Technol. **21**, 133 (1982).
[30] A. Amith, Phys. Rev. **139**, A1624 (1965).
[31] J. P. Dismukes, L. Ekstrom, E. F. Steigmeier, I. Kudman, and D. S. Beers, J. Appl. Phys. **35**, 2899 (1964).
[32] B. Abeles and R. W. Cohen, J. Appl. Phys. **35**, 247 (1964).
[33] T. Noguchi, *Proceedings of the 16th International Conference on Thermoelectrics* (IEEE Inc., Piscataway, NJ, 1997), p. 207.
[34] F. Edelman, M. Stoelzer, T. Raz, Y. Comem, C. B. Vining, H. Zeindl, and P. Zaumseil *Proceedings of the 16th International Conference on Thermoelectrics* (Ref. 33), p. 232.
[35] D. M. Rowe and V. S. Shukla, J. Appl. Phys. **52**, 7421 (1981).
[36] See V. I. Fistul', *Heavily Doped Semiconductors* (Plenum, New York, 1969), p. 145.
[37] T. H. Geball and G. W. Hull, Phys. Rev. **98**, 940 (1955).
[38] M. E. Brinson and W. Dunstan, J. Phys. C **3**, 483 (1970).
[39] J. O. Sofo and G. D. Mahan, Phys. Rev. B **49**, 4565 (1994).
[40] E. F. Steigmeier and B. Abeles, Phys. Rev. **136**, A1149 (1964).
[41] C. B. Vining, J. Appl. Phys. **69**, 331 (1991).
[42] G. A. Slack and M. A. Hussain, J. Appl. Phys. **70**, 2694 (1991).